

TEMPORAL AND SPATIAL SUMMATION IN THE HUMAN ROD VISUAL SYSTEM

By LINDSAY T. SHARPE, ANDREW STOCKMAN*, CLEMENS C. FACH
AND UWE MARKSTÄHLER

*From the Neurologische Universitätsklinik, Hansastrasse 9, D-7800 Freiburg im
Breisgau, FRG and the *Department of Psychology, University of California at
San Diego, La Jolla, CA 92093-0109, USA*

(Received 13 December 1991)

SUMMARY

1. Absolute and increment thresholds were measured in a retinal region 12 deg temporal from the fovea with 520 nm targets of varying size and duration. Measurements were made under rod-isolation conditions in two normal observers and in a typical, complete achromat observer who has no cone-mediated vision. The purpose of these experiments was to determine how the temporal and spatial summation of rod-mediated vision changes with light adaptation.

2. The absolute threshold and the rise in increment threshold with background intensity depend upon target size and duration, but the psychophysically estimated dark light of the eye (the hypothetical light assumed to be equivalent to photoreceptor noise) does not.

3. The rise in increment threshold for tiny (10 min of arc), brief (10 ms) targets approaches the de Vries–Rose square-root law, varying according to the quantal fluctuations of the background light. The slope of the rod increment threshold *versus* background intensity (TVI) curves in logarithmic co-ordinates is about 0.56 ± 0.04 (when cones are not influencing rod field adaptation). For large (6 deg) and long (200 ms) targets, a maximum slope of about 0.77 ± 0.03 is attained.

4. The steeper slopes of the rod-detected TVI curves for large, long targets implies some reduction in temporal or spatial summation. In fact, the change in summation area is much more critical: under conditions where only the rod system is active the TVI curve slope is independent of target duration, suggesting that temporal summation is practically independent of background intensity.

5. The rise in threshold also depends on the wavelength of the background field in the normal observer but not in the achromat, confirming reports that the field adaptation of the rods is not independent of the quantal absorptions in the cones. The cone influence is most conspicuous on long-wavelength backgrounds and is found for all target sizes and durations, but is greater for large and long targets than for the other conditions.

INTRODUCTION

These experiments concern the changes in temporal and spatial summation that occur as the isolated human rod visual system light adapts. To estimate the extent of such changes, we compare rod increment threshold *versus* background intensity (TVI) functions obtained with rod targets of different duration and size. It is well known that increasing target size or duration steepens the slopes of TVI functions (e.g. Stiles & Crawford, 1934; Graham & Kemp, 1938; Bouman, 1950; Barlow, 1957, 1958), and this has often been taken as evidence that spatial and temporal summation decreases as the visual system light adapts (but see Chen, MacLeod & Stockman, 1987, and the Discussion, below).

Previous studies of changes in temporal and spatial summation have employed procedures in which threshold is determined either primarily by cones (e.g. Graham & Kemp, 1938) or by rods at low adapting levels and by cones at higher levels (e.g. Stiles & Crawford, 1934; Bouman, 1950; Barlow, 1958), with – in most cases – no explicit attempt being made to distinguish rod from cone thresholds. As a result, the changes in summation inferred from these studies often confound changes in summation that occur under scotopic conditions with those that occur under photopic conditions.

It is important to look at the changes that occur under pure scotopic conditions because of the differences that underlie the human rod and cone visual systems. Not only do primate rod and cone photoreceptors vary in their dynamic responses to light (e.g. Baylor, Nunn & Schnapf, 1984; Schnapf, Nunn, Meister & Baylor, 1990), but also rod signals have access to a distinct pathway to the retinal ganglion cells, which is unavailable to cone signals and which is the primary visual pathway at low scotopic luminances (see Daw, Jensen & Brunken, 1990 for a recent review). Thus, photoreceptor isolation is likely to reveal differences in summation and adaptation that are postreceptoral as well as receptoral in origin.

In this study, we were careful to distinguish rod from cone thresholds. Only data measured well below the cone plateau thresholds following a rod bleach or data measured in a typical, complete achromat who displays no signs of functioning cone vision are used to estimate changes in temporal and spatial summation.

Additional precautions are necessary, if we are to use TVI functions to estimate changes in summation in the isolated rod system since it is well known that cones can raise rod threshold (e.g. Makous & Boothe, 1974). For example, under conditions similar to those used in the classic ‘rod isolation’ study of Aguilar & Stiles (1954), we have shown that a long-wavelength field steepens the logarithmic slope of the rod-mediated TVI curve for a 6 deg, 200 ms flash by nearly 20% compared to slopes measured on rod-equated shorter wavelength fields, even though target detection is mediated by rods (Sharpe, Fach, Nordby & Stockman, 1989*a*; Sharpe, Fach & Stockman, 1992).

To control for this cone intrusion, we obtain rod threshold data on short and middle wavelength backgrounds ($\mu = 450, 520$ and 560 nm), where rod sensitivity below the cone plateau is controlled almost exclusively by rods (Sharpe *et al.* 1992), and compare them with curves obtained on long-wavelength backgrounds ($\mu = 640$ nm), where rod sensitivity is strongly influenced by the cones. Additionally, we

exploit the rod threshold data of an achromat, which is free of cone influence, as a reference.

Applying such procedures yields a surprising result that deviates from conventional wisdom: increasing target duration has little effect on the slope of rod-mediated TVI curves below 1 scotopic troland (td). This suggests that there is little change in temporal summation with background intensity (see also Hallett, 1971). Increasing the target diameter, on the other hand, causes a substantial increase in the slopes of rod-mediated TVI curves.

METHODS

Subjects

Three male subjects were tested in these experiments, K.N. and authors C.F. and U.M. They were all informed about the nature of the experiment and that no risk to their health was involved. C.F. and U.M. are normal trichromats with normal (uncorrected) visual acuity. K.N. is a typical, complete achromat, who displays all the classic symptoms of typical, complete achromatopsia, without any evidence for cone function (for details, see Sharpe & Nordby, 1990). During the experiments, he wore a +9.0 dioptre convex lens, which magnified the retinal image 1.22 times. Thus, all of the visual angles in K.N.'s external field of view have to be corrected by this factor to bring them into agreement with visual angles in the uncorrected emmetropic eye.

Stimuli

Our experimental conditions were essentially the same as those used in the previous paper (Sharpe *et al.* 1992). The target and adapting field parameters were chosen to favour the rods relative to the cones – an unnecessary precaution in the achromat. The target had a wavelength of 520 nm. It was presented 12 deg extrafoveally (in the nasal field of view) in the centre of an 18 deg diameter, adapting field; and it entered the edge of the dilated pupil (3 mm off-centre) to take advantage of the Stiles–Crawford effect, which is much larger for the cones than for the rods (e.g. Stiles, 1939). The entry point of the adapting field was central. The duration and the size of the target was varied; as was the wavelength of the adapting field. It was either 450, 520, 560 or 640 nm.

Apparatus

The stimuli were seen in a four-channel Maxwellian view, optical system, interfaced with a computer (see Sharpe *et al.* 1992). In these experiments, only two channels were required: one to provide the target (incremental) stimulus; the other the adapting field.

The duration of the test flashes was controlled by a computer-operated electromagnetic shutter cutting a filament image in the target channel. The shutter had rise and fall times of less than 0.1 ms.

At the beginning and end of each experimental session, the quantal flux densities of the light beams were measured at the Maxwellian image with a silicon Pin-10 diode coupled to an operational amplifier (United Detector Technology, Model 80X Optometer, Orlando, FL, USA).

Procedure

About 30 min before beginning each experimental session, the subject had his left pupil dilated with 0.5% tropicamide (Mydraticum Roche®). He then positioned himself in the optical system by biting into a silicone-base, dental-wax impression of his teeth mounted in a machine tool-rest. Following 40 min of dark adaptation, he fixated a small illuminated cross placed so that the test flash and the adapting field were centred 12 deg on the temporal retina. The observer's absolute threshold was then measured several times by a computer-controlled, single staircase procedure. Threshold was defined as the mean wedge setting of twelve staircase reversals. At each new level the observer was pre-adapted for at least 3 min, before his threshold was determined. The

procedure continued until a full series of increment thresholds were obtained for a wide range of adapting field radiances. Such series were collected for all combinations of target durations, size and background wavelength.

In order to assess the extent of rod isolation for each background intensity (and wavelength), thresholds were also measured during the plateau that terminates the cone phase of recovery from a white (3100 K) bleaching light of $7.7 \log_{10}$ photopic troland seconds (td s).

TABLE 1. Rod incremental threshold responses for a 520 nm target of varying size and duration: absolute thresholds and dark noise values for a typical, complete achromat K.N. and two normal trichromat observers U.M. and C.F. estimated using eqn (1) (see text)

	Field wavelength, μ (nm)	U.M. (normal)	C.F. (normal) (\log_{10} scotopic td)	K.N. (achromat)
6 deg diameter, 200 ms duration				
Absolute threshold (mean \pm s.d.)		-3.65 ± 0.03	-4.09 ± 0.03	-3.39 ± 0.06
Dark noise	450	-3.79	-3.77	-2.87
	520	-3.85	-3.57	-2.57
	560	-3.50	-3.65	-2.71
	640	-3.60	-3.58	-2.99
	Mean \pm s.d.	-3.69 ± 0.16	-3.64 ± 0.09	-2.79 ± 0.18
6 deg diameter, 10 ms duration				
Absolute threshold (mean \pm s.d.)		-2.98 ± 0.10	-2.80 ± 0.10	-2.48 ± 0.09
Dark noise	450	-3.77	-3.66	-2.77
	520	-3.60	-3.15	-2.72
	560	-3.51	-3.61	-2.92
	640	-2.99	-3.66	-3.00
	Mean \pm s.d.	-3.47 ± 0.34	-3.52 ± 0.25	-2.85 ± 0.13
10 min of arc diameter, 200 ms duration				
Absolute threshold (mean \pm s.d.)		-1.15 ± 0.07	-1.51 ± 0.08	-1.28 ± 0.05
Dark noise	450	-3.39	-3.95	-2.49
	520	-3.84	-3.66	-2.91
	560	-3.02	-3.37	-2.62
	640	-3.74	-3.34	-2.72
	Mean \pm s.d.	-3.48 ± 0.37	-3.58 ± 0.29	-2.67 ± 0.18
10 min of arc diameter, 10 ms duration				
Absolute threshold (mean \pm s.d.)		-0.39 ± 0.02	-0.44 ± 0.13	-0.29 ± 0.09
Dark noise	450	-3.82	-3.39	-2.95
	520	-3.73	-3.46	-2.84
	560	-3.42	-3.51	-2.72
	640	-3.61	-3.88	-3.53
	Mean \pm s.d.	-3.67 ± 0.21	-3.56 ± 0.22	-3.01 ± 0.36
Average dark noise (mean)		-3.58	-3.58	-2.83

Data treatment

Slope. To determine the slopes of the rod detected portions of the increment threshold curves, the thresholds were fitted by means of a computerized curve-fitting program (Sigmaplot, Jandel Scientific, Corte-Madera, CA, USA) using the logarithmic form of the following equation:

$$\Delta I = k(I_{\mu} + I_0)^n. \quad (1)$$

In eqn (1), ΔI is the increment threshold intensity and I_{μ} is the background field intensity of wavelength μ . I_0 is a 'dark light' constant added to account for the levelling off of the increment threshold curve at low background intensities; it determines the point at which the slope of the

increment threshold curve rises above the asymptotic absolute threshold value. Changing the value of I_0 has the effect of shifting the curve laterally along the $\log_{10} I_\mu$ axis. The exponent n is the asymptotic slope and k is a vertical positioning constant (kI_0^n corresponds to the absolute threshold tabulated in Table 1, below).

For each individual observer, the fitting of eqn (1) to the increment threshold data was completed in two stages. In the first stage, the three parameters, I_0 , k and n , were allowed to vary freely and individual fits were determined for each of the TVI curves measured against the four (450, 520, 560 and 640 nm) field wavelengths m . Since the values for k for each observer did not vary with μ (i.e. absolute threshold is independent of adapting field wavelength) and those for I_0 did not vary with μ or with target condition (see Table 1, below), average values were applied in the second fitting stage. In the final fits to the sixteen TVI curves only n was allowed to vary.

In both fitting procedures, eqn (1) was fitted to the threshold data from absolute threshold to a background on which threshold still lies clearly below the cone plateau thresholds. For each observer, the fits at 450, 520 and 560 nm (and the secondary fit at 640 nm, see below) were made over the same range of background intensities. This range was increased at 640 nm, since rod isolation extends to higher scotopic intensities at that wavelength. In general, the upper limit was an increment threshold lying at least 0.5 \log_{10} unit below cone threshold. The range of background intensities over which each fit was made is indicated by the horizontal extent of the continuous curves shown in Figs 1-3.

Temporal and spatial integration. To determine the extent of the change in spatial or temporal integration, we measured thresholds with targets of two diameters (6 deg and 10 min of arc) and two durations (10 and 200 ms).

Traditionally, the range of sizes over which threshold is inversely proportional to the target size (i.e. when Ricco's law holds; Ricco, 1887) is taken to be the range over which there is complete spatial summation, and the range of durations over which the threshold is inversely proportional to the target duration (i.e. when Bloch's law holds; Bloch, 1885) is taken to be the range over which there is complete temporal summation (but see Discussion). The 6 deg and 200 ms targets that we used were considered large and long enough to exceed the upper limits of complete spatial (estimated to be between 0.5 and 2 deg; see, for example, Barlow, 1958) and temporal (estimated to be about 100 ms; see Fig. 5, below) summation of rod-mediated vision, even in the dark. The 10 min of arc and 10 ms targets were considered small and brief enough to be within the limits of complete spatial and temporal summation of rod-mediated vision, even at the highest background intensities. We note that the 200 ms target may fall within the region where temporal summation is only partial, at least for small fields (Barlow, 1958; and Fig. 5, below).

We first averaged the 450, 520 and 560 nm TVI data for each normal observer within 0.5 \log_{10} unit bins. (The 640 nm TVI data were separately analysed to determine how the concomitant desensitization of the cones affects the estimates of rod temporal and spatial integration.) Data points were only included between the adapting field intensities corresponding to I_0 (see Table 1) and the level at which the cones mediate threshold. (In the achromat K.N., the full extent of the curves could be used, so two separate analyses were made: one included data up to an adapting intensity at which cone intrusion occurs in the normal observer, the other included data up to rod saturation. His data were averaged over all four background wavelengths.) The data for the appropriate target conditions were then subtracted from each other and the remainders were fitted by simple linear regression equations to yield the following estimates:

'Total' or the combined temporal and spatial change:

$$(10 \text{ min of arc, 10 ms thresholds}) - (6 \text{ deg, 200 ms thresholds});$$

S_{long} or the spatial change for long duration targets:

$$(10 \text{ min of arc, 200 ms thresholds}) - (6 \text{ deg, 200 ms thresholds});$$

S_{brief} or the spatial change for brief duration targets:

$$(10 \text{ min of arc, 10 ms thresholds}) - (6 \text{ deg, 10 ms thresholds});$$

T_{large} or the temporal change for large diameter targets:

$$(6 \text{ deg, 10 ms thresholds}) - (6 \text{ deg, 200 ms thresholds});$$

T_{small} or the temporal change for small diameter targets):

$$(10 \text{ min of arc, 10 ms thresholds}) - (10 \text{ min of arc, 200 ms thresholds}).$$

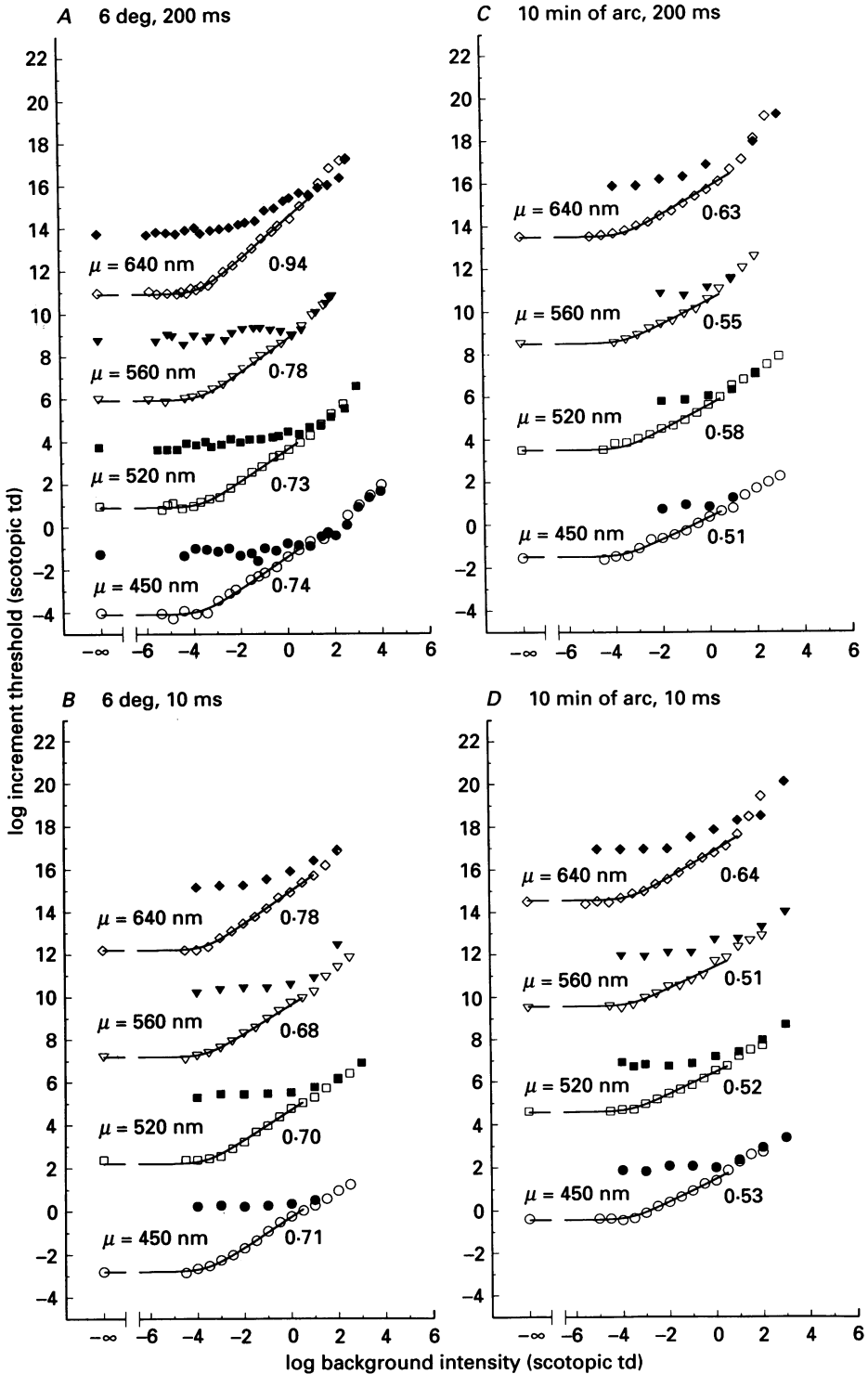


Fig. 1. For legend see facing page.

RESULTS

Absolute threshold

Table 1 lists, for the four target conditions, each observer's absolute threshold, estimated according to eqn (1). Expressed in terms of scotopic trolands, the absolute threshold increases as the target is made small and brief (the values given in Table 1 for each target condition are averaged over the four adapting field wavelengths). Expressed in terms of the total amount of light incident at the cornea, however, it is actually lowest for the tiny, brief target.

Absolute threshold for the tiny (10 min of arc), brief (10 ms) target requires approximately 41, 36 and 52 (507 nm) quanta incident at the cornea, respectively, for observers U.M., C.F. and K.N. These values are slightly lower than the 'classic' values reported by Hecht, Schlaer & Pirenne (1942). They found that for a tiny (10 min of arc), brief (1 ms) target between 54 and 148 incident quanta were required for threshold.

The comparable absolute threshold in quanta for the other targets are: 580 (U.M.), 440 (C.F.) and 1055 (K.N.) for the 6 deg, 200 ms target; 136 (U.M.), 205 (C.F.) and 429 (K.N.) for the 6 deg, 10 ms target; and 141 (U.M.), 62 (C.F.) and 105 (K.N.) for the 10 min of arc, 200 ms target. These larger values reflect the fact that the longer, larger targets exceed the upper limits of complete spatial and/or temporal summation.

Dark light

The absolute threshold is believed to be limited by internal noise within the visual system or the 'dark light' (Barlow, 1956, 1957). Estimates of each observer's dark light, I_0 in eqn (1), are listed in Table 1 for each target and adapting field condition (I_0 roughly accords with the background intensity corresponding to the intersection of the line of constant slope with the absolute threshold ordinate in Figs 1-3).

The estimates of I_0 are remarkably consistent across conditions for any one observer. For achromat K.N., the estimated dark light is $-2.83 \pm 0.24 \log_{10}$ scotopic td or 676 quanta (507 nm) $s^{-1} \text{deg}^{-2}$ at the cornea, which corresponds to a

Fig. 1. The effect of background wavelength (μ) on the form of the rod increment threshold *versus* intensity curve for normal observer C.F. The threshold curves were measured for four target conditions: 6 deg, 200 ms (A); 6 deg, 10 ms (B); 10 min of arc, 200 ms (C); 10 min of arc, 10 ms (D). In all conditions, the target had a wavelength of 520 nm and was presented 12 deg extrafoveally in the centre of an 18 deg diameter adapting field. It entered the edge of the dilated pupil (3 mm off-centre) to take advantage of the Stiles-Crawford effect. Four background wavelengths were used for each target conditions: 450 (○), 520 (□), 560 (▽) or 640 (◇) nm. The corresponding filled symbols represent the thresholds measured for the same stimulus conditions during the plateau that terminates the cone phase of recovery from a white (3100 K) bleaching light of $7.7 \log_{10}$ photopic td s. The curves are correctly placed with respect to the axis of the abscissae, but the axis of the ordinates is correct only for the lowest curve ($\mu = 450$ nm) in each of the four panels; the other curves are displaced upward in intervals of $5.0 \log_{10}$ units. Each data point is a mean based on at least three sets of measurements made on different days. The continuous lines drawn through each set of increment threshold data, below the point at which the cone plateau thresholds intersect the steady-state thresholds, are the best-fitting logarithmic forms of eqn (1). The slope (n) in logarithmic co-ordinates is shown to the right of each curve (see Table 2).

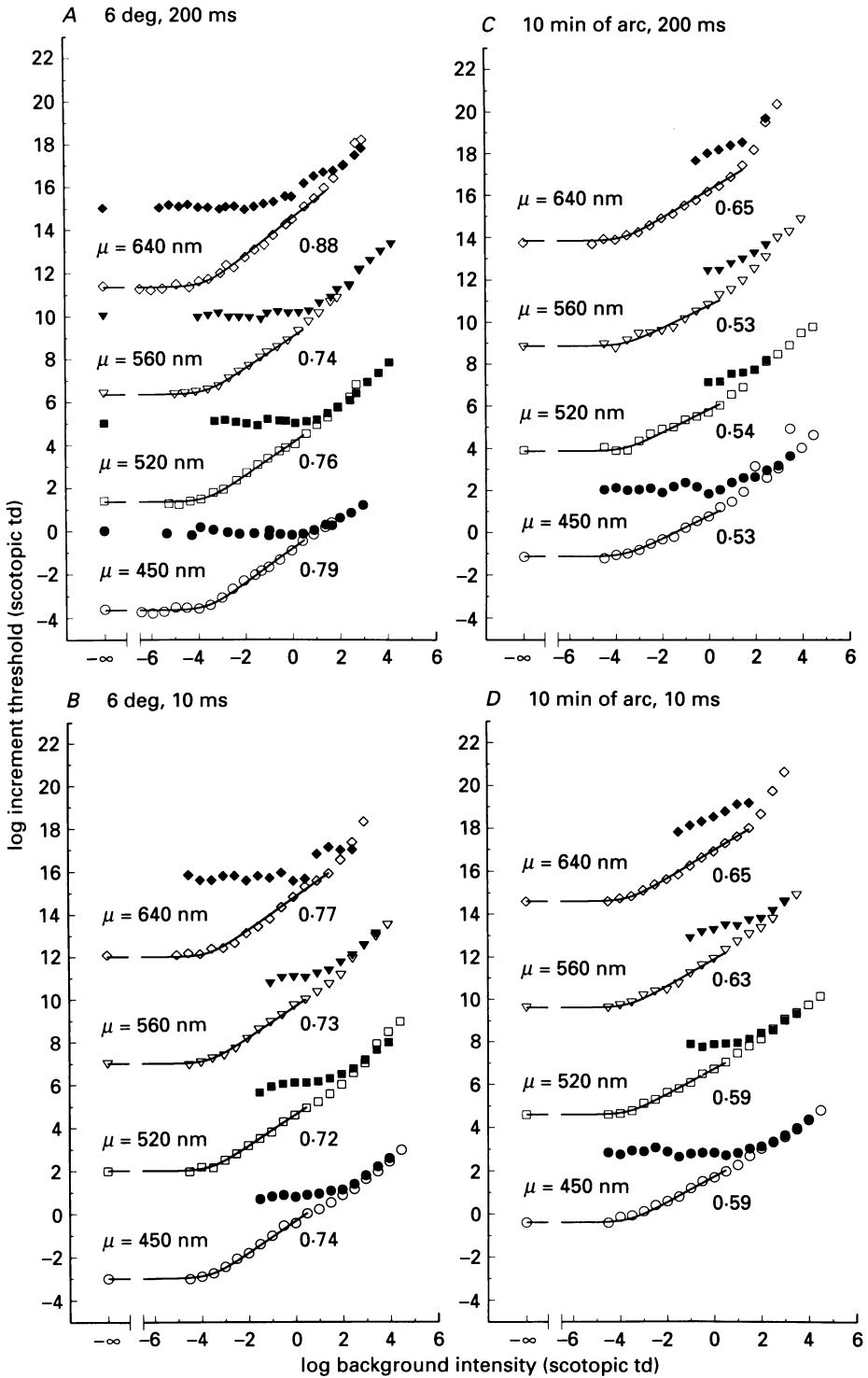


Fig. 2. For legend see facing page.

photoisomerization rate of approximately once every 92 s per rod. For normal observer C.F., it is $-3.58 \pm 0.20 \log_{10}$ scotopic td or 120 quanta (507 nm) s^{-1} deg, which corresponds to a photoisomerization once every 521 s per rod. For normal observer U.M., it is $-3.58 \pm 0.27 \log_{10}$ scotopic td or 120 quanta (507 nm) s^{-1} deg $^{-1}$, which corresponds to a photoisomerization once every 521 s per rod. The fact that the dark light of the normal observers is smaller than that of the achromat K.N. is consistent with their lower absolute thresholds.

Slope

Figures 1–3 present, for four background wavelengths, the increment threshold curves measured for the two normal observers, C.F. (Fig. 1) and U.M. (Fig. 2), and for the achromat observer K.N. (Fig. 3). Results are given for each of four target conditions: 6 deg, 200 ms (panel A); 6 deg, 10 ms (panel B); 10 min of arc, 200 ms (panel C) and 10 min of arc, 10 ms (panel D).

6 deg, 200 ms target

For the largest (6 deg), longest (200 ms) target (panel A), the results agree with those given in the preceding article (Sharpe *et al.* 1992, Figs 1–3). In the two normal observers, U.M. and C.F., there is a wavelength dependence in slope of the increment threshold curve with adapting field wavelength: the 640 nm background causes the rod threshold to rise more steeply than do the other backgrounds. The change can be assessed by comparing the final logarithmic slopes of the TVI functions; these are shown to the right of each set of increment threshold data. These slopes refer to the curves (continuous lines) fitted to the rod-detected increment thresholds, according to eqn (1). The final slopes are listed along with the other curve-fitting parameters in Table 2. In the achromat K.N., who has no cone vision, there is no dependence upon background wavelength. His slope is constant across wavelength, averaging 0.78 ± 0.04 against all backgrounds. For the normal observers it averages 0.75 ± 0.03 (C.F.) and 0.76 ± 0.02 (U.M.) against the 450, 520 and 560 nm backgrounds and is 0.94 (C.F.) and 0.88 (U.M.) against the 640 nm background.

It can be seen in Figs 1 and 2 that in the normal observers the rods determine threshold up to higher scotopic background intensities on the 640 nm background than on the shorter wavelength backgrounds. This allows us to fit eqn (1) over a more extended range of background intensities at 640 nm. To ensure that the increased slopes found at 640 nm are not entirely due to the inclusion of these higher intensity threshold data (for it could be that the slope simply increases with intensity), we also fitted eqn (1) over the same range of scotopic background intensities at 640 nm as we used for the fits at shorter wavelengths. The resulting slopes are tabulated in an additional row of Table 2 (this has also been done for the other target conditions). The slopes are still markedly higher at 640 nm than at shorter wavelengths even for the reduced fit.

Fig. 2. The effect of background wavelength (μ) on the form of the rod increment threshold *versus* intensity curve for normal observer U.M. Same conditions as in Fig. 1. The parameters of the continuous lines drawn through each set of increment threshold data are given in Table 2.

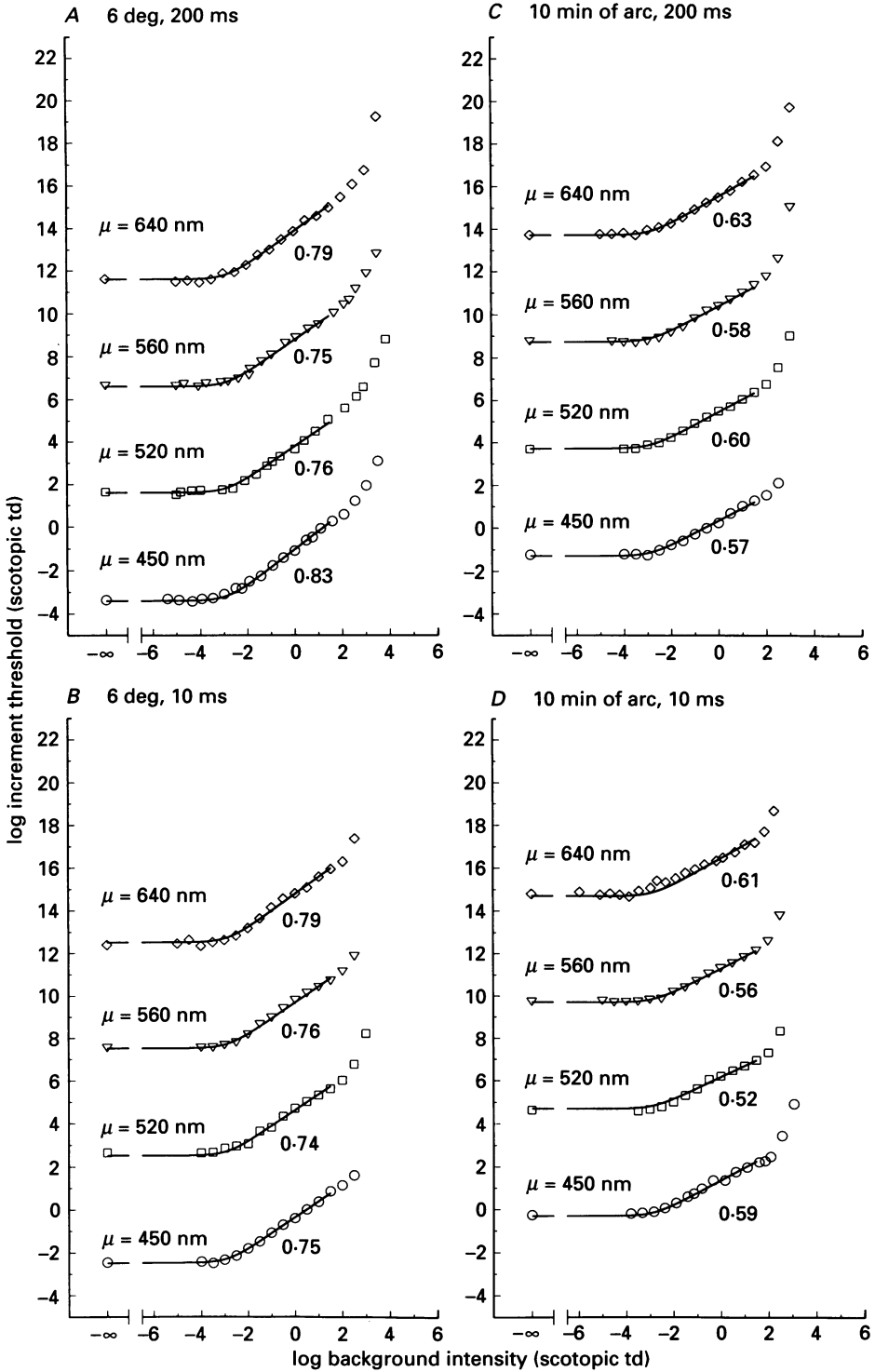


Fig. 3. For legend see facing page.

6 deg, 10 ms target

When the target duration is decreased to 10 ms (Figs 1–3, panel B), there is still a dependence of slope on background wavelength for normal observers, but it is weaker than for the 6 deg, 200 ms target. In the achromat, as before, the slope remains constant across wavelength. The slopes in both the normal and achromat observers

TABLE 2. Rod incremental threshold responses for a 520 nm target of varying size and duration: TVI slopes for a typical, complete achromat K. N. and two normal trichromat observers U.M. and C.F. estimated using eqn. (1) (see text) and the mean absolute thresholds and dark noise values listed in Table 1

Field wavelength, μ (nm)	U.M. (normal)	C.F. (normal)	K.N. (achromat)
6 deg diameter, 200 ms duration			
450	0.79	0.74	0.83
520	0.76	0.73	0.76
560	0.74	0.78	0.75
640	0.88	0.94	0.79
640*	0.86	0.93	—
6 deg diameter, 10 ms duration			
450	0.74	0.71	0.75
520	0.72	0.70	0.74
560	0.73	0.68	0.76
640	0.77	0.78	0.79
640*	0.74	0.78	—
10 min of arc diameter, 200 ms duration			
450	0.53	0.51	0.57
520	0.54	0.58	0.60
560	0.53	0.55	0.58
640	0.65	0.63	0.63
640*	0.62	0.61	—
10 min of arc diameter, 10 ms duration			
450	0.59	0.53	0.59
520	0.59	0.52	0.52
560	0.63	0.51	0.56
640	0.65	0.64	0.61
640*	0.64	0.62	—

* This row tabulates the 640 nm slopes estimated over the same range of background intensities for each subject as the 450, 520 and 560 nm slopes.

Fig. 3. The effect of background wavelength (μ) on the form of the rod increment threshold *versus* intensity curve for achromat observer K.N. Same conditions as in Fig. 1, except that no cone plateau thresholds could be measured for this observer. The parameters of the continuous lines drawn through each set of increment threshold data are given in Table 2.

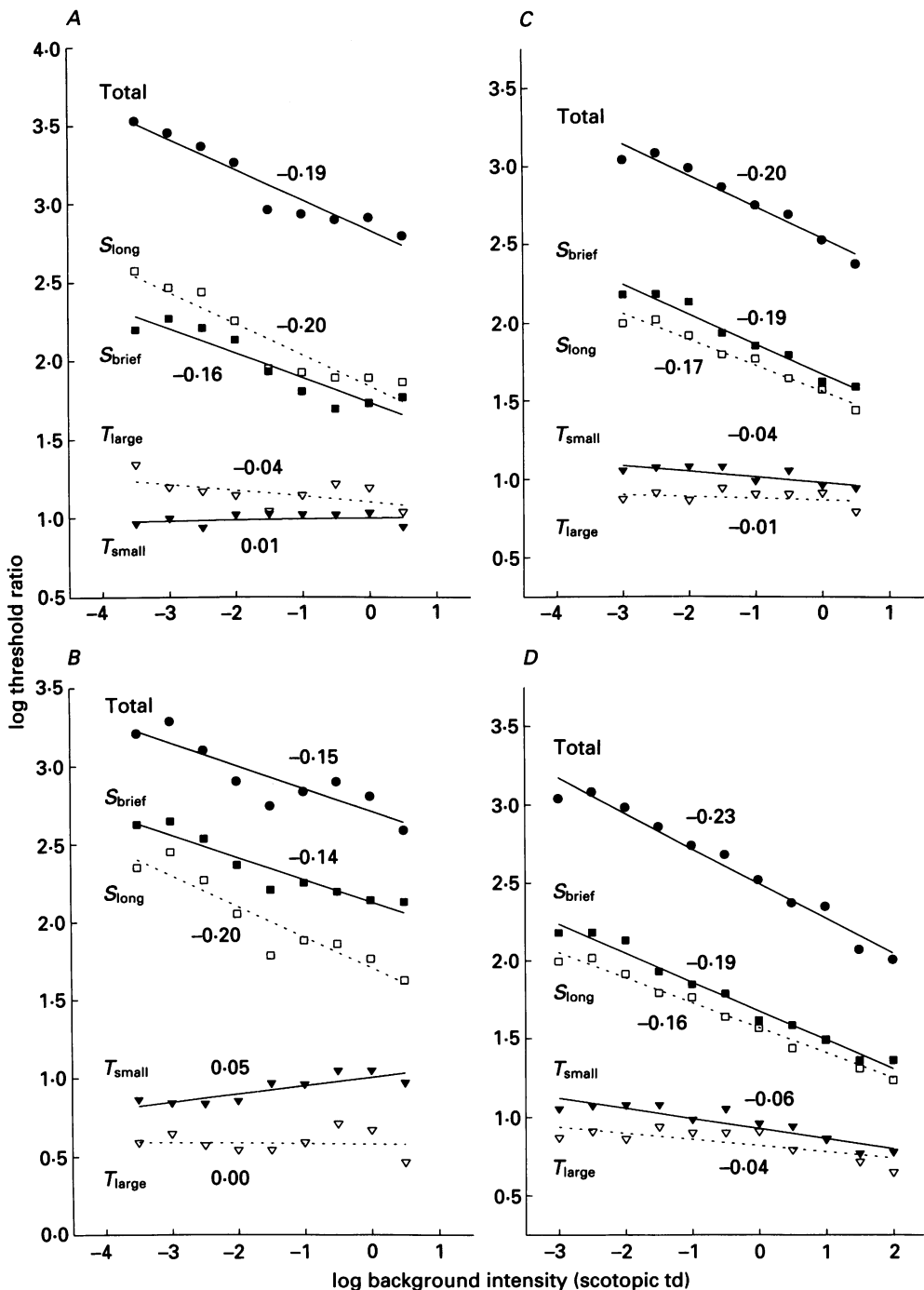


Fig. 4. Estimates of the change in the spatial and temporal summation of the rod visual system of the two normal observers C. F. (A) and U. M. (B) and the achromat K. N. (C) as a function of background intensity, from the intensity corresponding to the observer's dark light up to the intensity at which the cones start to influence threshold in normal observers (approximately $0.5 \log_{10}$ scotopic td). Also shown are the estimates of achromat

tend to be slightly less than those for the 200 ms test flash (see Table 2). In the normal observers, the average slope measured on all backgrounds other than 640 nm is 0.70 ± 0.02 (C.F.) and 0.73 ± 0.01 (U.M.) (*vs.* 0.75 and 0.76, respectively, for the 200 ms test flash condition); on the 640 nm background it is 0.78 (C.F.) and 0.77 (U.M.) (*vs.* 0.94 and 0.88, respectively). In the achromat, the slope on all backgrounds including 640 nm is 0.76 ± 0.02 (*vs.* 0.78). The small reduction in slope accords with the idea that increasing the background intensity reduces the time over which the rod visual system integrates light (Barlow, 1958). However, the effect (except for the 640 nm field in normals, for which the reduction is larger), if any, is very small.

10 min of arc, 200 ms target

Panel *C* of Figs 1–3 presents the field adaptation curves obtained when the target duration is kept long (200 ms), but the target diameter is reduced to 10 min of arc. This provides a measure of the influence of changes in spatial reorganization upon the rod field adaptation curve, which will influence the slope of the curve for a large flash but not for a small one if the size of the small target is smaller than the minimum summation area of the rod visual system. Reducing the target size clearly results in increment threshold curves of shallower slopes. For the achromat K.N., the slope has an average value of 0.60 ± 0.03 across wavelength (*vs.* 0.78 for the large, long target, see Table 2). For the normal observers, the slope on the 450, 520 and 560 nm backgrounds average 0.55 ± 0.04 (C.F.) and 0.53 ± 0.01 (U.M.) (*vs.* 0.75 and 0.76), but are 0.63 (C.F.) and 0.65 (U.M.) (*vs.* 0.93 and 0.86) on the 640 nm background.

10 min of arc, 10 ms target

Panel *D* of Figs 1–3 presents the field adaptation curves obtained when the target duration is shortened to 10 ms and the target diameter reduced to 10 min of arc. Jointly reducing target duration and size does not markedly further decrease the slope of the curves compared to reducing the size alone (see Table 2). For the achromat K.N., the slope has an average value of 0.57 ± 0.04 across wavelength. For the normal observers, the slopes on the 450, 520 and 560 nm backgrounds average 0.52 ± 0.01 (C.F.) and 0.60 ± 0.02 (U.M.). On the 640 nm background, the slopes are 0.62 (C.F.) and 0.64 (U.M.).

K.N. determined over an extended adapting field range (*D*), including levels up to those corresponding to the onset of rod saturation. 'Total' (combined temporal and spatial change) is the log ratio of the observer's threshold quantity of light for a 10 ms, 10 min of arc diameter target to his threshold intensity for a 200 ms, 6 deg diameter target. T_{small} (temporal summation for small flashes) is the log ratio of the observer's threshold quantity of light for the 10 ms, 10 min of arc diameter target to his threshold intensity for the 200 ms, 10 min of arc diameter target. T_{large} (temporal summation for large flashes) is the log ratio of the observer's threshold quantity of light for the 6 deg diameter, 10 ms target to his threshold intensity for the 6 deg diameter, 200 ms target. S_{brief} (spatial summation for brief flashes) is the log ratio of the observer's threshold quantity of light for the 10 ms, 10 min of arc diameter target to his threshold intensity for the 10 ms, 6 deg diameter target. S_{long} (spatial summation for long flashes) is the log ratio of the observer's threshold quantity of light for the 200 ms, 10 min of arc diameter target to his threshold intensity for the 200 ms, 6 deg diameter target. The threshold ratios for normal observers C.F. and U.M. were averaged over the 450, 520 and 560 nm background data; those for achromat K.N. over the 640 nm data as well.

Additional targets

The slope values listed in Table 2 are roughly confirmed by additional values measured for normal observer U.M. when the target diameter was held constant at 0.3 deg, but the target duration was decreased from 100 to 20 ms. Slopes were determined for two adapting field wavelengths, 450 and 640 nm (The slopes were determined from graphic plots and not according to eqn (1)). On the 450 nm background, where rods are predominantly desensitized (or activated), all slopes roughly approximate 0.50, regardless of target duration: 0.53 (100 ms), 0.45 (70 ms), 0.48 (50 ms) and 0.50 (20 ms). On the 640 nm background, however, where cones contribute to desensitization by the background as well, the slopes are significantly higher than 0.5 for all target durations: 0.68 (100 ms), 0.65 (70 ms), 0.62 (50 ms), 0.60 (20 ms).

Estimates of spatial and temporal summation

Figure 4 provides an estimate for each observer of the change in the spatial and temporal summation of the rod visual system as a function of background intensity. First, it plots the effect of the combined change in temporal and spatial summation (labelled 'Total'); that is, the log ratio of each observer's threshold quantity of light for the 10 ms, 10 min of arc (0.022 deg²) target to his threshold intensity for the 200 ms, 6 deg (28.27 deg²) target (from Figs 1-3). For achromat K.N., the comparison has been made over the same adapting field range as for the normal observers (i.e. from the adapting field intensity corresponding to the dark noise up to the intensity level at which the cones start to influence threshold in the normal observers, approximately 0.5 log₁₀ scotopic td). It has also been made over an extended adapting field range (i.e. up to the adapting field intensity corresponding to the onset of rod saturation, approximately 2.0 log₁₀ scotopic td) to determine if further temporal and spatial reorganization occurs in the rod visual system at intensity levels where the rod responses are normally masked by those of the cones.

The comparison assumes that changes in temporal and spatial summation do not affect the 10 ms, 10 min of arc threshold because the target area and duration are always within the ranges where complete temporal and spatial summation occur, but that the changes affect the 200 ms, 6 deg threshold because the target area and duration exceed these ranges as the adapting level is increased. It can be seen that the amount of total summation change is similar for all three observers, decreasing as the powers 0.20 (K.N.), 0.19 (C.F.) 0.15 (U.M.), as the background intensity is raised from about -3.5 (normal observers) or -3.0 (achromat K.N.) to 0.5 log₁₀ scotopic td. An additional small change may be occurring at higher intensities because the value measured for K.N. over the extended range (from about -3.0 to 2.0 log₁₀ scotopic td) is slightly larger (0.23). The reduction in summation causes an overall threshold elevation by factors of 5.0 (K.N.), 14.1 (K.N., extended range), 5.8 (C.F.) and 4.0 (U.M.).

These values for the exponent change are similar to that (0.25) reported by Barlow (1958), when he compared thresholds measured in normal observers for a 7.5 ms, 0.0077 deg² target and a 935 ms, 19 deg² target.

Second, the figure plots the change in spatial summation for each observer for brief flashes (labelled S_{brief}); that is, the log ratio of the observer's threshold quantity of

light for the 10 ms, 10 min of arc target to his threshold intensity for the 10 ms, 6 deg target. As the background intensity is raised, the amount of spatial summation for all three observers decreases by powers of 0.19 (K.N.), 0.19 (K.N., extended range), 0.16 (C.F.) and 0.14 (U.M.). Over the same intensity range, threshold correspondingly rises by factors of 4.6 (K.N.), 8.9 (K.N., extended range), 4.4 (C.F.) and 3.6 (U.M.) in area.

Third, Fig. 4 plots for each observer the change in spatial summation for long flashes (labelled S_{long}); that is, the log ratio of each observer's threshold quantity of light for the 200 ms, 10 min of arc target to his threshold intensity for the 200 ms, 6 deg target. As the background intensity is raised, the amount of summation for all three observers decreases by powers of 0.17 (K.N.), 0.16 (K.N., extended range), 0.20 (C.F.) and 0.20 (U.M.), corresponding to threshold factor rises of 3.9 (K.N.), 6.3 (K.N., extended range), 6.3 (C.F.) and 6.3 (U.M.). There is little difference between the S_{brief} and S_{long} estimates, suggesting that the change in spatial summation is roughly independent of target duration.

Fourth, Fig. 4 plots the change in temporal summation for each observer measured with small flashes (labelled as T_{small}); that is, the log ratio of each observer's threshold quantity of light for the 10 ms, 10 min of arc target to his threshold intensity for the 200 ms, 10 min of arc target. As the background intensity is raised, the amount of temporal summation for all three observers changes by powers of -0.04 (K.N.), -0.06 (K.N., extended range), 0.01 (C.F.) and 0.05 (U.M.), corresponding to threshold factor changes of 1.4 (K.N.), 2.0 (K.N. extended range), 1.1 (C.F.) and 1.6 (U.M.).

Finally, the figure plots the change in temporal summation for each observer measured with large diameter targets (labelled as T_{large}); that is, the log ratio of each observer's threshold quantity of light for the 10 ms, 6 deg target to his threshold intensity for the 200 ms, 6 deg target. As the background intensity is raised, the amount of temporal summation for all three observers changes by powers of -0.01 (K.N.), -0.04 (K.N. extended range), -0.04 (C.F.) and 0.00 (U.M.), corresponding to threshold factor changes of 1.1 (K.N.), 1.6 (K.N., extended range) 1.4 (C.F.) and 1.0 (U.M.). That there is virtually no difference between the T_{small} and T_{large} estimates suggests that the change in temporal summation - what little there is - is independent of target size.

DISCUSSION

In general accord with Barlow (1957), we find that thresholds determined with a tiny, brief target rise less quickly with adaptation than those determined with a large, long target. The former, measured in the achromat or in the normal observers for $\mu \leq 560$ nm (see Table 2), rise with an average slope of 0.57 (± 0.04), and the latter with a slope of 0.77 (± 0.03). This difference in slope is conventionally taken to reflect a reduction of the visual system's temporal and spatial summation capability with light adaptation. The tiny, brief target is assumed to be unaffected by the intensity-dependent changes in summation, since it is always within the limits of complete summation. But, because the larger and longer targets exceed those limits, they show an accelerated loss of sensitivity with light adaptation.

At first glance, then, our data seem consistent with the notion that the visual system sacrifices sensitivity at higher levels for improvements in temporal and spatial resolution. However, in the achromat and in the normal observer for $\mu \leq 560$ nm, the average TVI slope is only $0.56 (\pm 0.04)$ for the 10 min of arc, 200 ms

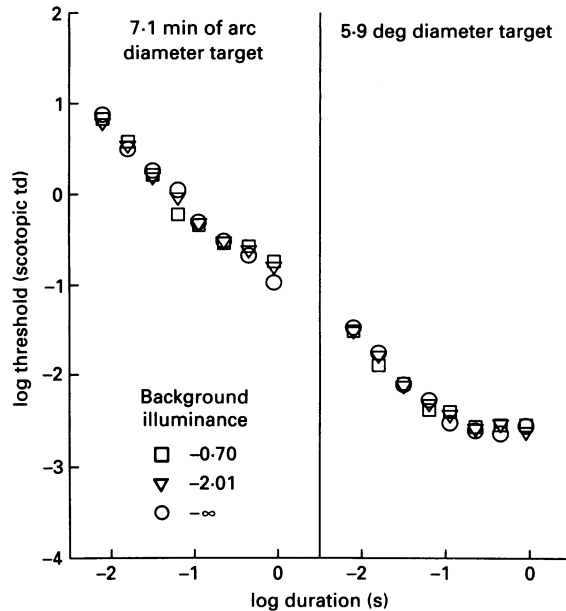


Fig. 5. Scotopic temporal summation estimates from Barlow (1958; his Fig. 2). The two panels show log increment threshold intensity plotted against log duration for small (7.1 min of arc, left panel) and large (5.9 deg, right panel) diameter rod-detected targets at three adapting field illuminances, $-\infty$, -2.01 and -0.70 scotopic td. The three sets of data in each panel have been shifted vertically, so that the thresholds superimpose (for details, see text).

flash. This is nearly identical to the average slope for the briefer, 10 min of arc, 10 ms flash (0.57 ± 0.04). Similarly, the average TVI slope for the 6 deg, 200 ms flash (0.77 ± 0.03) is very similar to the average slope for the briefer 6 deg, 10 ms flash (0.73 ± 0.04). Clearly, these TVI slopes show little dependence on target duration, suggesting that within the range of our measurements there is only a small change of temporal integration with light adaptation. Thus, below $0.5 \log_{10}$ scotopic td, the rod visual system does not sacrifice sensitivity for improvements in temporal resolution.

This is made clear in Fig. 4, where we plot the differences between the thresholds obtained with the four targets. From the regression lines fitted to the data in Fig. 4, we conclude that there is a 4–5.8 change in threshold due to both spatial and temporal factors, a 3.6–4.6 change due to spatial factors alone and a 1.0–1.5 change due to temporal factors alone. Thus, the decline in sensitivity due to changes in target size is about 3 times greater than that due to changes in its duration. The decline in rod temporal summation is surprisingly small and is not significantly

enhanced by extending the range of adapting luminance (K.N.'s data in Fig. 4 suggest that there is only a small additional change in temporal integration for rod-mediated vision at luminances between 0.0 and $2.0 \log_{10}$ scotopic td).

The change in temporal summation with light adaptation

When detection is mediated by rods, our data, therefore, give little support for the traditional assumption that there is a large change in temporal integration with adaptation. It is curious that no-one has apparently challenged this assumption before, especially since an examination of the previously published data reveals little evidence for a change in temporal integration for rod-mediated vision below $0.5 \log_{10}$ scotopic td (however, see Hallett, 1971; his Fig. 7).

Take, for instance, the frequently cited temporal summation measurements of Barlow (1958). Barlow used homochromatic target and adapting conditions (497 nm), so that rod-isolated target detection and field adaptation can be safely assumed for his three lowest adapting levels, $-\infty$, 3.65 and $4.96 \log_{10}$ quanta (507 nm) $s^{-1} \text{ deg}^{-2}$ (corresponding to $-\infty$, -0.70 and $-2.01 \log_{10}$ scotopic td). Barlow's original TVI thresholds measured with 7.1 min of arc (0.011 deg^2) and 5.9 deg (27.6 deg^2) targets, replotted from his Fig. 2, are shown in Fig. 5, shifted vertically to minimize the squared deviations between them. When so shifted, they superimpose almost exactly. This indicates that changes in temporal summation cannot be significantly influencing the thresholds; for otherwise clear differences in shape would be found. Bouman (1950) made similar measurements to those of Barlow shown here; and an examination of them yields a similar conclusion. If Barlow's (1958) data shown in Fig. 5 are shifted to minimize the squared-deviations only for durations of less than 100 ms (the leftmost points in each panel, where Bloch's Law holds), there are minor differences at longer durations that might indicate a small reduction in temporal integration, but only for durations greater than 500 ms.

Another example is Lennie (1979), who measured TVI curves in one subject for 0.2 deg, 15 ms; 0.2 deg, 1 s; 7.5 deg, 15 ms; and 7.5 deg, 1 s targets. He, like us, found that the TVI slope was independent of target duration: it was 0.5 for the 0.2 deg target, and 0.83 for the 7.5 deg target. Curiously, Lennie does not comment on the fact that his results suggest that there is no change in temporal integration for rod-mediated vision with light adaptation. Instead, he speculates that the change in spatial integration is caused by a decrease in the latency of the receptive field surround. But if that were the case, the rod-mediated TVI slopes would not be independent of target duration.

Previous measurements of TVI functions in the same achromat observer as used in this study also imply very small changes in temporal summation with light adaptation. Stabell, Nordby & Stabell (1987) measured K.N.'s TVI curves with a 520 nm, 1×2 deg diameter target of varying duration. An examination of their Fig. 3 reveals no change in slope for targets measured with 8 ms, 125 ms and 1 s flashes.

One study that does show evidence for a change in temporal integration for rod-mediated vision is the elegant two-target work of van den Brink & Bouman (1954). They find a change in temporal integration in the scotopic range (see their Fig. 2). But the effect is small: over the whole scotopic *and* photopic range the change in

temporal summation decreases threshold by a factor of only 1.8 (van den Brink & Bouman, 1954; p. 620).

As mentioned above, the data shown in Fig. 4 suggest that temporal integration for rod-mediated vision may start to decline at mesopic luminances above $0.0 \log_{10}$ scotopic td. This change in temporal summation may be related to the transition

TABLE 3. The slopes of incremental threshold *versus* intensity curves measured for achromat K.N.

Target diameter (deg)	Target area (deg ²)	Target duration (ms)	Slope (log-log co-ordinates)
6.00‡	28.30	200	0.78 ± 0.04
6.00†	28.30	200	0.77 ± 0.02
6.00‡	28.30	10	0.76 ± 0.02
1.85§	2.69	200	0.73
1 × 2*	2.00	1000	0.70
1 × 2*	2.00	125	0.67
1.85§	2.69	50	0.68
1.00‡	0.79	100	0.67
1 × 2*	2.00	8	0.65
0.17§	0.02	200	0.63
0.17‡	0.02	200	0.58 ± 0.02
0.20*	0.03	125	0.62
0.17§	0.02	50	0.59
0.17‡	0.02	10	0.57 ± 0.04

* Stabell *et al.* (1987).

† Sharpe, Fach, Nordby & Stockman (1989*a*).

‡ Present paper.

§ Sharpe, Whittle & Nordby (1993).

from the slow rod pathway, π_0 , to the faster pathway, π'_0 , which can be clearly identified in both psychophysical and electrophysiological flicker data (e.g. Stockman, Sharpe, Zrenner & Nordby, 1991). The temporal frequency response and the phase characteristics of the slow rod pathway, which predominates below $0.0 \log_{10}$ scotopic td, suggest that the time constant of the slow rod pathway changes little with light adaptation. In contrast, the time constant of the faster pathway, which predominates at mesopic levels, may shorten with light adaptation (Sharpe, Stockman & MacLeod, 1989*b*). The transition between detection by slow and fast rod pathways seems to depend surprisingly little on temporal frequency (Sharpe *et al.* 1989*b*; see their Fig. 9), and so will be more or less independent of target duration.

A dramatic change in the time constant of the photopic cone system with light adaptation can be easily demonstrated (e.g. Kelly, 1961). Thus, our results point to a major difference in the sensitivity regulation of the scotopic and photopic visual systems.

Changes in spatial integration with light adaptation

Our finding of a change in spatial summation as the human rod visual system light adapts accords with the findings of many other workers (e.g. Bouman, 1950; van den Brink & Bouman, 1954; Barlow, 1958; Lennie, 1979). Parallel changes have been found for extra-foveal thresholds measured with 2.7 min of arc and 7 deg diameter

fields during the rod-mediated portion of the dark-adaptation curve; that is, the rate of dark adaptation was found to increase with the size of the target (Arden & Weale, 1954).

In the achromat, other TVI measurements also suggest a change in spatial integration with light adaptation. Blakemore & Rushton (1965) measured increment threshold in a rod-monochromat with 1 s duration, achromatic flashes of large and small target diameter. They found that the curve measured with a small (5 min of arc) diameter flash rose with a slope of 0.59, whereas that measured with a large (6 deg) diameter flash rose with a slope of 0.87. Stabell *et al.* (1987) measured TVI curves in the same achromat as used in this study with a 520 nm, 125 ms flash of varying diameter. An examination of their fig. 2 reveals a change in slope between the thresholds measured with a small (0.2 deg) and large (1 × 2 deg) diameter target. Table 3 lists how the slope of achromat K.N.'s increment threshold curves depends upon target size and duration. It summarizes the data obtained here and in earlier publications. Clearly, the effect of reducing the size of the target has a greater effect on the slope than reducing the duration of the target.

Other explanations of the steepening of rod-mediated TVI curves with target size

A local adaptation-dependent non-linearity

Chen *et al.* (1987) have argued that the change in the slopes of TVI curves with target size can be explained by strictly local processes. As an illustration of their model, consider the targets used in the experiments reported here: the small, 10 min of arc target and the large, 6 deg target differ not only in size, but also in the luminance required to detect them. Thus, *locally*, the 10 min of arc target produces a much larger response at threshold than the 6 deg target. If light adaptation increases the steepness of the function relating stimulus intensity to local response (the local input-output function), the threshold for the larger target will rise more steeply with adaptation than the threshold for the smaller one, without any need to invoke changes in spatial integration (Chen *et al.* 1987; see their Fig. 1). The experiments of Chen *et al.*, which were directed mainly at cone vision, showed that there was little change in spatial integration with light adaptation. Sharpe *et al.* (1993) have recently repeated the experiments of Chen *et al.* in the achromat observer, K.N. Their results suggest that there is a change in spatial integration in the rod visual system during light adaptation, over and above that due to local changes, but that it is small.

Spatial filters

Another explanation of the change in the slopes of TVI curves with target size is one based on the model of the early visual system as several channels sensitive to different spatial frequencies (e.g. Campbell & Robson, 1968), each with independent gain controls (e.g. Enroth-Cugell & Shapley, 1973). The TVI curves for the large, 6 deg target could be steeper than the TVI curves for the small, 10 min of arc target, if the high spatial frequency channels detecting the 10 min of arc target suffer less desensitization in bright light than do the low spatial frequency channels detecting the 6 deg target (Enroth-Cugell & Shapley, 1973; Hess, 1990). This argument is complicated by the fact that our sharply focused, 6 deg target is spatially broadband,

and so might be detected by channels tuned to low spatial frequencies at low intensities and high spatial frequencies at high intensities. It remains true, however, that the multichannel model is essentially inconsistent with the results of Chen *et al.* (1987), and is difficult to reconcile with the simple reciprocity of stimulus intensity and target size found for small target sizes (though, see Hess, 1990, Fig. 1.8).

The cone influence on long-wavelength fields

So far, we have discussed the isolated rod system. In the normal observer, however, it has been shown by several workers that the cones can raise rod threshold (see above). A secondary aim of this work was to determine how the cone influence on rod threshold depends on target size and duration.

This issue has also been considered by Makous & Peeples (1979), who measured the cone elevation of the rod detection threshold for 20 ms duration targets of various diameters ranging from 2 min of arc to 1 deg. They found no systematic change in the size of the rod-cone interaction with target size. However, they also measured the cone elevation for rod detected, 200 ms targets of 1 deg diameter or 1 deg square, and found that the rod-cone interaction was slightly larger for these larger and longer targets than for any of the 20 ms targets (0.38 *vs.* 0.29 \log_{10} unit).

Like Makous & Peeples (1979), we find that the increase in rod increment threshold on long-wavelength backgrounds is greater than on rod-equated short- and middle-wavelength backgrounds – irrespective of the target size and/or duration. The difference in slope between the TVI curves for $\mu \leq 560$, and those for $\mu = 640$ nm ranges from 0.04 to 0.18. There seems to be no particular pattern to these results, except that, consistent with the findings of Makous & Peeples (1979), – the increase in slope for the TVI curves obtained with the 6 deg, 200 ms target is greater than that for the TVI curves obtained with the other targets. This suggests that there is a spatio-temporal interaction when cones influence rod threshold. Such interactions have been discussed by Barlow (1958), who attributes them to a sluggish lateral inhibition in the retina, which must be greater for long than for brief targets. Perhaps, then, cone adaptation raises rod threshold by introducing a sluggish lateral inhibition.

The limits of ‘complete’ spatial and temporal summation

As the target is made larger and longer, more quanta are required to detect it at absolute threshold (see Table 1 and Results above). This has been observed by many workers (see Hecht *et al.* 1942), and can be explained by the inefficiency of targets whose size or duration extends beyond the spatial and temporal limits within which there is a reciprocity between stimulus area and intensity (Ricco, 1887) and between stimulus duration and intensity (Bloch, 1885). At absolute threshold in the peripheral retina, the spatial limit of complete summation is typically assumed to be between 30 min of arc and 2 deg in diameter, and the temporal limit of complete summation is assumed to be about 100 ms. But estimates of complete spatial and temporal summation vary widely and depend upon stimulus configuration and retinal eccentricity (for a review, see Sharpe, 1990).

We can estimate the upper limits of spatial and temporal summation implied by our TVI data by assuming an abrupt transition from complete summation to no

summation. In the dark-adapted eye, the upper limits estimated from our data are 58, 117 and 98 ms for U.M., C.F. and K.N., respectively, for temporal summation, and 3.4, 2.6 and 2.1 deg for spatial summation.

These estimates ignore the fact that beyond the limits of complete spatial and temporal summation there is a region of partial summation ($\Delta I = k_1/A^n$ and $\Delta I = k_2/T^m$, $0 < n < 1$; where ΔI represents detection threshold, A the target area, T the target duration, and k_1 and k_2 are constants; Ricco's and Bloch's laws correspond to $n = 1$) (e.g. Barlow 1958).

Cohn (1990) has recently reiterated that if quantum fluctuations limit incremental detection, complete summation does not correspond to Ricco's law or Bloch's laws, but instead to the range of sizes or durations for which $\Delta I = k_1/A^{0.5}$ or $\Delta I = k_2/T^{0.5}$ (see also Piper, 1903; van der Velden, 1944; Barlow, 1964). According to this model, Ricco's and Bloch's law correspond to sizes and durations where the stimuli are detected *less efficiently* due to the counting of too many quanta from the background (Barlow, 1964). This argument, however, is valid only if detection is actually limited by quantum fluctuations. As Cohn points out (Cohn, 1990, p. 380), the fact that the three square-root laws of temporal summation, spatial summation, and background intensity (the de Vries-Rose law) do not co-exist in Barlow's (1958) data (see Cohn, 1990, his Fig. 33.2) suggests that detection is not limited by quantum fluctuations.

Dark light, I_0

The so called 'dark light' has been attributed to the spontaneous thermal activations of rhodopsin molecules, which are assumed to be indistinguishable from photo-elicited events (e.g. Barlow, 1956, 1957, 1958; Baylor *et al.* 1984; Aho, Donner, Hyden, Reuter & Orlov, 1987). Baylor *et al.* (1984) have determined that the thermal isomerization rate in individual monkey rods is about once every 160 s, which corresponds to 390 quanta (507 nm) $s^{-1} \text{ deg}^{-2}$ being presented to the cornea (for a discussion of this point, see Sharpe, 1990; and for a discussion of dark light in cat retinal ganglion cells, see Shapley & Enroth-Cugell, 1984). In support of this explanation, a firm link has been established between the rate of thermal isomerizations and the performance limit of visually guided behaviour in the dark-adapted frog and toad (Aho *et al.* 1987) and, in the human, it has been observed that the absolute threshold rises with body temperature, roughly according to the relationship between thermal isomerization rate and temperature (Fach & Sharpe, 1990).

Estimates of dark light are roughly constant within an observer, but, as is already well known, vary considerably between observers. Barlow (1957) found estimates in the literature differing by a factor of 80, from 200 to 16000 quanta (507 nm) $s^{-1} \text{ deg}^{-2}$ at the cornea (see his Table 1). Because some of the larger estimates were imprecise he concluded that the true variance is closer to a factor of 16 and that a reasonable average value is about 1000 quanta (507 nm) $s^{-1} \text{ deg}^{-2}$ ($-2.66 \log_{10}$ scotopic td). This corresponds to about one photoisomerization every 62 s, according to the conversion factors given in Sharpe (1990, pp. 59-60). Other studies give values of 200-1300 quanta (506 nm) $s^{-1} \text{ deg}^{-2}$ or about one photoisomerization every 48-313 s (Aguilar & Stiles, 1954), 400 quanta (507 nm) $s^{-1} \text{ deg}^{-2}$ or about one photoisomerization every 156 s (Hallett, 1969), and 50-200 quanta (507 nm) $s^{-1} \text{ deg}^{-2}$ or one photoisomer-

ization every 312–1250 s (Sakitt, 1972). The range in our observers is from 676 (K.N.) to 120 (U.M.) quanta (507 nm) $s^{-1} \text{deg}^{-2}$ at the cornea; corresponding to a photoisomerization rate of from once every 92 s to once every 521 s per rod.

The analysis of our TVI data suggests that target size and duration do not significantly affect estimates of the intrinsic dark light of the eye (see Table 1). But, since there is little or no change in temporal integration with light adaptation, we should expect I_0 to be independent of target duration – as indeed it is. The finding that I_0 is independent of target size is more unexpected. There are several reasons why this might be so. One possibility is that there may be no change in spatial summation at light intensities equivalent to the dark light levels. Another is that the source of the dark light noise may originate at a stage beyond the early stages of spatial integration.

Physiological evidence

Our psychophysical data show that the slopes of rod-mediated TVI curves depend more on changes in target area than on changes in target duration. Comparable TVI curves have been derived from cat retinal ganglion cell recordings by plotting the amplitude of the cell response divided by the stimulus strength (i.e. the retinal ganglion cell gain) *versus* the background level.

In the scotopic range, the relation of the slope to target parameters follows the same pattern as that observed psychophysically. Thus, Barlow & Levick (1976) report that, for large-area (usually 4.6 deg), long-duration (0.32–1.26 s) targets, slopes of single units average 0.82 and approach 1.0 in the steepest cases, whereas for small (10 min of arc), long-duration (1 s) targets the slopes average 0.58 and for small (less than the receptive field centre size), brief (10 ms) targets, the slopes average about 0.53. Likewise, Lennie (1979) reports that the slopes for large stimuli covering the whole receptor field are steeper (1.2–1.4) than those for small stimuli falling within the centre of the receptive field (0.65).

There are several noteworthy aspects of these findings. First, the slopes found by Barlow & Levick in the cat conform surprisingly well to those given in Table 2 for, for example, achromat K.N.: 0.77 ± 0.03 for the large, long test flash; 0.56 ± 0.04 for the small, long one; and 0.57 ± 0.04 for the small, brief one. The slopes found by Lennie in the cat, however, are steeper than those measured psychophysically in K.N. The significance of this difference is complicated by the fact that the method of determining threshold for a ganglion cell influences the shape of the increment threshold curve. For instance, the slope of the increment threshold curve can be reduced by optimizing the analysis period (see Lennie, 1979).

Second, the results of both Barlow & Levick (1976) and Lennie (1979) indicate that changes in target duration have less effect on the ganglion cell thresholds than changes in target area (though curiously neither reported this). This accords with the psychophysical thresholds presented above and suggests that changes in spatial summation of cells are more important than changes in temporal summation. Changes in spatial summation with light adaptation have been directly measured in the excitatory receptive field centre of cat retinal ganglion cells and have been shown to be between 32 and 50% over a 4.5 to 5.0 \log_{10} unit range (Enroth-Cugell & Robson, 1966; Derrington & Lennie, 1982).

This research was supported by the Alexander von Humboldt-Stiftung, Bonn-Bad Godesberg, by the Deutsche Forschungsgemeinschaft (SFB 325, B4 & B13 and Heisenberg-Programme), Bonn-Bad Godesberg, and by the National Science Foundation (BNS 88-12401). The visit of K.N. was made possible by funds received from the Research Division of the Norwegian Telecommunication Administration. We thank Drs D. I. A. MacLeod and P. Whittle for advice and comments.

REFERENCES

- AGUILAR, M. & STILES, W. S. (1954). Saturation of the rod mechanism at high levels of stimulation. *Optica Acta* **1**, 59–65.
- AHO, A.-C., DONNER, K., HYDEN, C., REUTER, T. & ORLOV, O. Y. (1987). Retinal noise, the performance of retinal ganglion cells and visual sensitivity in the dark-adapted frog. *Journal of the Optical Society of America A* **4**, 2321–2329.
- ARDEN, G. B. & WEALE, R. A. (1954). Nervous mechanism and dark adaptation. *Journal of Physiology* **125**, 417–426.
- BARLOW, H. B. (1956). Retinal noise and absolute threshold. *Journal of the Optical Society of America* **46**, 634–639.
- BARLOW, H. B. (1957). Increment thresholds at low intensities considered as signal/noise discriminations. *Journal of Physiology* **136**, 469–488.
- BARLOW, H. B. (1958). Temporal and spatial summation in human vision at different background intensities. *Journal of Physiology* **141**, 337–350.
- BARLOW, H. B. (1964). The physical limits of visual discrimination. In *Photophysiology*, vol. II, ed. GIESE, A. C., pp. 163–202. Academic Press, New York.
- BARLOW, H. B. & LEVICK, W. R. (1976). Threshold settings by the surround of cat retinal ganglion cells. *Journal of Physiology* **259**, 737–757.
- BAYLOR, D. A., NUNN, B. J. & SCHNAPF, J. L. (1984). The photocurrent, noise and spectral sensitivity of rods of the monkey *Macaca fascicularis*. *Journal of Physiology* **357**, 575–607.
- BLAKEMORE, C. B. & RUSHTON, W. A. H. (1965). Dark adaptation and increment threshold in a rod monochromat. *Journal of Physiology* **181**, 612–628.
- BLOCH, A. M. (1885). Expériences sur la vision. *Société Biologie Memoir* (Paris) **37**, 493–495.
- BOUMAN, M. A. (1950). Peripheral contrast thresholds of the human eye. *Journal of the Optical Society of America* **40**, 825–832.
- CAMPBELL, F. W. & ROBSON, J. G. (1968). Application of Fourier analysis to the visibility of gratings. *Journal of Physiology* **197**, 551–566.
- CHEN, B., MACLEOD, D. I. A. & STOCKMAN, A. (1987). Improvement in human vision under bright light: grain or gain? *Journal of Physiology* **394**, 41–66.
- COHN, T. E. (1990). Spatial and temporal summation in human vision. In *Vision: Coding and Efficiency*, ed. BLAKEMORE, C., chap. 33, pp. 376–385. Cambridge University Press: Cambridge.
- DAW, N. W., JENSEN, R. J. & BRUNKEN, W. J. (1990). Rod pathways in mammalian retinae. *Trends in Neurosciences* **13**, 110–115.
- DERRINGTON, A. M. & LENNIE, P. (1982). The influence of temporal frequency and adaptation level on receptive field organization of retinal ganglion cells in cat. *Journal of Physiology* **333**, 343–366.
- ENROTH-CUGELL, C. & ROBSON, J. G. (1966). The contrast sensitivity of retinal ganglion cells of the cat. *Journal of Physiology* **187**, 517–522.
- ENROTH-CUGELL, C. & SHAPLEY, R. M. (1973). Flux, not retinal illumination, is what cat retinal ganglion cells really care about. *Journal of Physiology* **233**, 311–326.
- FACH, C. C. & SHARPE, L. T. (1990). Absolute threshold and body temperature. *Investigative Ophthalmology and Visual Science* **31**, suppl. 413.
- GRAHAM, C. H. & KEMP, E. H. (1938). Brightness discrimination as a function of the duration of the increment in intensity. *Journal of General Physiology* **21**, 635–650.
- HALLETT, P. E. (1969). Quantum efficiency and false positive rate. *Journal of Physiology* **202**, 421–436.
- HALLETT, P. E. (1971). Rapid changes and hysteresis in spatial integration for human rod vision. *Journal of Physiology* **215**, 433–447.
- HECHT, S., SHLAER, S. & PIRENNE, M. H. (1942). Energy, quanta and vision. *Journal of General Physiology* **25**, 819–840.

- HESS, R. F. (1990). Rod-mediated vision: role of post-receptor filters. In *Night Vision: Basic, Clinical and Applied Aspects*, ed. HESS, R. F., SHARPE, L. T. & NORDBY, K., chap. 1, pp. 3–48. Cambridge University Press, Cambridge.
- KELLY, D. H. (1961). Visual responses to time-dependent stimuli. I. Amplitude sensitivity measurements. *Journal of the Optical Society of America* **51**, 422–429.
- LENNIE, P. (1979). Scotopic increment thresholds in retinal ganglion cells. *Vision Research* **19**, 425–430.
- MAKOUS, W. L. & BOOTHE, R. (1974). Cones block signals from rods. *Vision Research* **14**, 285–294.
- MAKOUS, W. L. & PEEPLES, D. R. (1979). Rod–cone interaction: reconciliation with Flamant and Stiles. *Vision Research* **19**, 695–698.
- PIPER, H. (1903). Über die Abhängigkeit des Reizwertes leuchtender Objekte von ihre Flächen- bzw. Winkelgrasse. *Zeitschrift für Psychologie und Physiologie der Sinnesorgane* **32**, 98–112.
- RICCO, A. (1877). Relazione fra il minimo angolo visual e l'intensità luminosa. *Memorie della Regia Accademia di Scienze, lettere ed arti in Modena* **17**, 47–160.
- SAKITT, B. (1972). Counting every quantum. *Journal of Physiology* **233**, 131–150.
- SCHNAFF, J. L., NUNN, B. J., MEISTER, M. & BAYLOR, D. A. (1990). Visual transduction in cones of the monkey *Macaca fascicularis*. *Journal of Physiology* **427**, 681–713.
- SHAPLEY, R. M. & ENROTH-CUGELL, C. (1984). Visual adaptation and retinal gain control. In *Progress in Retinal Research*, vol. 3, ed. OSBORNE, N. O. & CHANDLER, G. J., chap. 9, pp. 263–346. Pergamon Press, Oxford.
- SHARPE L. T. (1990). The light-adaptation of the human rod visual system. In *Night Vision: Basic, Clinical and Applied Aspects*, ed. HESS, R. F., SHARPE, L. T. & NORDBY, K., pp. 49–124. Cambridge University Press, Cambridge.
- SHARPE, L. T., FACH, C. C., NORDBY, K. & STOCKMAN, A. (1989*a*). The incremental threshold of the rod visual system and Weber's law. *Science* **244**, 354–356.
- SHARPE, L. T., FACH, C. C. & STOCKMAN, A. (1992). The field adaptation of the human rod visual system. *Journal of Physiology* **445**, 319–343.
- SHARPE, L. T. & NORDBY, K. (1990). The photoreceptors in the achromat. In *Night Vision: Basic, Clinical and Applied Aspects*, ed. HESS, R. F., SHARPE, L. T. & NORDBY, K., pp. 335–389. Cambridge University Press, Cambridge.
- SHARPE, L. T., STOCKMAN, A. & MACLEOD, D. I. A. (1989*b*). Rod flicker perception: scotopic duality, phase lags and destructive interference. *Vision Research* **29**, 1539–1559.
- SHARPE, L. T., WHITTLE, P. & NORDBY, K. (1993). Spatial integration and sensitivity changes in the human rod visual system. *Journal of Physiology* **461**, 235–246.
- STABELL, B., NORDBY, K. & STABELL, U. (1987). Light-adaptation of the human rod system. *Clinical Vision Sciences* **2**, 83–91.
- STILES, W. S. (1939). The directional sensitivity of the retina and the spectral sensitivities of the rods and cones. *Proceedings of the Royal Society B* **127**, 64–105.
- STILES, W. S. & CRAWFORD, B. H. (1934). The liminal brightness increment for white light for different conditions of the foveal and parafoveal retina. *Proceedings of the Royal Society B* **116**, 55–102.
- STOCKMAN, A., SHARPE, L. T., ZRENNER, E. & NORDBY, K. (1991). Slow and fast pathways in the human rod visual system: electrophysiology and psychophysics. *Journal of the Optical Society of America A* **8**, 1657–1665.
- VAN DEN BRINK, G. & BOUMAN, M. A. (1954). Variation of integrative actions in the retinal system: an adaptational phenomenon. *Journal of the Optical Society of America* **44**, 616–620.
- VAN DER VELDEN, H. (1944). Over het aantal lichtquata dat nodig es for en licht prikkel bij dat menselyk oog. *Physica* **11**, 179–189.